

1 Sexual antagonism drives the displacement of polymorphism across gene  
2 regulatory cascades

3 Mark S. Hill<sup>1,2</sup>, Max Reuter<sup>\*2</sup> & Alexander J. Stewart<sup>\*\*3</sup>

4 <sup>1</sup> Department of Ecology and Evolutionary Biology, University of Michigan, Ann Arbor, MI, USA

5 <sup>2</sup> Research Department of Genetics, Evolution and Environment, University College London, London, United  
6 Kingdom

7 <sup>3</sup> Department of Biology & Biochemistry, University of Houston, Houston, TX, USA

8 \* Email: m.reuter@ucl.ac.uk

9 \*\* Email: astewar6@central.uh.edu

10 **Keywords:** Sexual antagonism, gene regulation, binding site, transcription factor, regulatory  
11 cascade

## 12 Abstract

13 Males and females have different reproductive roles and are often subject to contrast-  
14 ing selection pressures. This sexual antagonism can lead, at a given locus, to different  
15 alleles being favoured in each sex and, consequently, to genetic variation being main-  
16 tained in a population. Although the presence of sexually antagonistic polymorphisms  
17 has been documented across a range of species, their evolutionary dynamics remain  
18 poorly understood. Here we study sexually antagonistic selection on gene expression,  
19 which is fundamental to sexual dimorphism, via the evolution of regulatory binding  
20 sites. We show that for sites longer than 1 nucleotide, expression polymorphism is  
21 maintained only when intermediate expression levels are deleterious to both sexes. We  
22 then show that, in a regulatory cascade, expression polymorphism tends to become  
23 displaced over evolutionary time from the target of sexually antagonistic selection to  
24 upstream regulators. Our results have consequences for understanding the evolution  
25 of sexual dimorphism, and provide specific empirical predictions for the regulatory  
26 architecture of genes under sexually antagonistic selection.

## 27 Introduction

28 Adaptive responses to divergent selection in males and females are hampered by a largely shared  
29 genome, which slows or even prevents the evolution of sexual dimorphism, where the two sexes  
30 reach their respective phenotypic optima. In this situation populations can experience the invasion  
31 of “sexually antagonistic” (SA) alleles that are beneficial in one sex, but deleterious in the other  
32 [1, 2, 3, 4].

33 Sexual antagonism is increasingly recognised as a taxonomically widespread and evolutionarily  
34 important phenomenon. A wealth of empirical evidence for SA fitness variation across a wide range  
35 of animal and plant species has now accumulated [5, 6, 7, 8, 9, 10, 11]. Sexual antagonism is thought  
36 to be a key driver for the evolution of sex chromosomes [12, 13] and sex determination [14, 15, 16],  
37 to play a role in reproductive evolution (by eroding “good genes” benefits of sexual selection [17]),  
38 and to mitigate the evolution of reproductive conflict between the sexes [18]. More generally, sexual  
39 antagonism has been predicted to maintain alleles in balanced polymorphism [19] and thus may  
40 also contribute to the maintenance of genetic and fitness variation within populations [20, 21] and  
41 a reduction in the evolvability of both sexes [22].

42 The conditions that favor emergence and maintenance of SA variation in a population have been  
43 explored by a large body of theoretical work. These previous models have captured the fate of SA  
44 variation in infinite populations [1, 23] under a wide range of dominance effects [24], in the presence  
45 of genetic drift in finite populations [25, 26], under fluctuating environments [27], and when there  
46 is selection on linked SA polymorphisms [19, 28]. What they all have in common, however, is that  
47 they consider small numbers of allelic variants at one or a small number of loci (often a single  
48 bi-allelic locus).

49 It is important to realise that the abstract concept of the ‘locus’ in these models imposes  
50 limitations on the applicability and generality of their results. Specifically, the notion of alleles  
51 segregating at distinct and unlinked loci makes the implicit assumption that variants with SA fit-  
52 ness effects can arise by simple, individual mutation events. This is appropriate when considering  
53 SA selection on protein coding sequences, where non-synonymous substitutions can generate evo-  
54 lutionary relevant phenotypic variation in males and females. However, the assumption of isolated  
55 polymorphisms breaks down in the case of regulatory evolution, where the phenotype—and hence

56 fitness—is determined by the match between the sequence of a putative binding site and the motif  
57 that is recognised by a transcription factor. Here, it is the combination of sequence states at all  
58 positions of a binding site that matters, rather than the state at any individual position. The  
59 degeneracy of individual regulatory sequences typifies regulatory evolution but, in the framework  
60 of existing models of sexual antagonism, would imply complex effects of linkage and epistasis that  
61 cannot be readily analysed. Accordingly, previous models are of limited use to predict SA evolution  
62 of gene regulation.

63     Developing models which allow us to explore the evolution of gene regulation under SA selec-  
64 tion is an important goal, because SA selection on regulatory regions is all but inevitable. This  
65 inevitability arises because sexual dimorphism requires the differential use, and hence expression,  
66 of genes in males and females and therefore can only arise via a period of opposing selection on gene  
67 regulation between the sexes [29]. Understanding how sexually dimorphic regulation can evolve,  
68 and the constraints that may oppose its evolution, necessitates models that can adequately describe  
69 the evolution of regulatory binding sites under sex-specific selection.

70     To model binding site evolution in this way, we here build on previous work that considers  
71 the fitness landscape of sequence states across the entire binding site by integrating the known  
72 biophysical properties of TF binding into models of regulatory evolution. These models often  
73 make the simplifying assumption that each nucleotide within a binding site contributes equally and  
74 independently to that site’s binding energy. While in reality this may not always be true [30, 31],  
75 these models are considered to appropriately capture the evolutionary dynamics of gene regulation  
76 [30, 32, 33, 34, 35, 36].

77     We extend these models to study the effects of SA selection on cis-regulatory evolution. We  
78 explore, via simulation and analysis, the selective conditions that permit invasion and maintenance  
79 of SA binding site variants in a population. We then expand our modeling framework to consider  
80 regulatory cascades under SA selection, and determine where in a regulatory chain polymorphisms  
81 are most likely to arise and persist. We show that regulatory architecture has a fundamental impact  
82 on our expectations about the selective conditions, and the positions within a regulatory network,  
83 that give rise to SA polymorphisms. We further show that SA selection can lead to ongoing reor-  
84 ganisations in regulatory cascades over evolutionary timescales, including abrupt “displacement”  
85 events, where the location of polymorphism shifts from genes directly under SA selection, to one

86 of their upstream regulators.

## 87 **Materials and Methods**

88 Here we describe the details of the biophysical and population genetic model used to generate our  
89 results. Transcription factor binding sites are typically around 10 nucleotides long in eukaryotes [35],  
90 while the population-scaled mutation rate in *Drosophila* is  $N_e u \sim 0.01$  (where  $N_e$  is the effective  
91 population size and  $u$  is the mutation rate per nucleotide site [37]) and an order of magnitude  
92 lower in humans, placing both species in the weak mutation limit. For simplicity in our simulations  
93 (which vary population size, binding site length and the number of binding sites) we assume a  
94 “standard” binding site of length  $n = 10$  and set the per-binding-site mutation rate at  $\mu = 10u$ .  
95 We then run all of our simulations with  $N_e \mu = 0.1$ , which keeps all of our simulations in the weak  
96 mutation limit [37, 38].

## 97 **Gene Expression**

98 The biophysics of transcription factor binding is well approximated by assuming an optimal consen-  
99 sus sequence, such that each nucleotide in a contiguous sequence of  $n$  nucleotides can be considered  
100 as either “matched” to the consensus sequence or not. Below we refer to the number of matched  
101 nucleotides as  $k$ , with a matched nucleotide independently contributing an amount,  $\epsilon \sim 1 - 3k_B T$   
102 (absolute energy units) [30, 31], to the site’s binding energy. The probability  $\pi_k$  that a binding site  
103 consisting of  $k$  matched nucleotides is bound by a TF protein is given by

$$\pi_k = \frac{P}{P + \exp[\epsilon(n - k)]}$$

104

105 where  $P$  is the number of TF proteins available to bind to the site. We assume  $P = 200$  in our  
106 simulations. The rate of transcription (for a fixed decay rate) and the number of translated proteins  
107 at the target for a site that up-regulates expression can then be treated, to a first approximation,  
108 as proportional to the probability that the binding site is bound. If we define the expression  $E$  of  
109 the target gene as the number of expressed proteins proportional to the maximum, we have simply

$$E = \frac{P}{P + \exp[\epsilon(n - k)]} \quad (1)$$

110

111 This expression assumes that the TF is an activator, meaning stronger binding results in higher  
 112 expression levels, with expression  $E$  varying between a minimum  $E \sim 0$  and a maximum  $E \sim 1$ .  
 113 Note that the scale here is arbitrary, since we are not directly modelling the process of transcription  
 114 and translation, we are simply assuming that stronger binding corresponds to higher expression.  
 115 Similarly, we could consider the case of a repressor, in which case  $E$  would decrease with  $k$ , and  
 116 our results apply equally to this type of regulation.

117 Mutations to binding sites are assumed to occur via single nucleotide substitutions, such that  
 118 the probability of increasing the number of matches by 1, from  $k \rightarrow k + 1$ , is  $u(n - k)/3$  where the  
 119 factor 3 reflects the fact that only one out of the three possible nucleotide changes will correctly  
 120 match to the consensus sequence. Similarly the rate of mutations that decrease the number of  
 121 nucleotide matches by 1, from  $k \rightarrow k - 1$  is  $uk$ . We therefore not only have a multi-allele system  
 122 but one with asymmetric forward and back mutations, which makes analytical treatment difficult  
 123 in most cases.

124 Since we are considering diploid organisms each individual carries two alleles, 1 and 2, with two  
 125 expression levels  $E_1$  and  $E_2$ , so that overall expression of the gene in each individual is given by  
 126  $E = (E_1 + E_2)/2$ . This simplifying assumption of additivity is well supported with several studies  
 127 finding that cis-regulatory alleles tend to have additive effects on gene expression [39, 40].

## 128 **Fitness Landscape**

129 To explore SA selection over gene expression in this framework we assume that the gene under  
 130 SA selection favors binding that results in maximally high expression ( $E \sim 1$ ) given the TF input  
 131  $P$  (complete binding) in males and maximally low expression given  $P$  (no binding,  $E \sim 0$ ) in  
 132 females. As we note above however, expression level  $E$  is arbitrary under our model and our results  
 133 correspond to any case where selection favors higher expression in one sex and lower, (including  
 134 non-zero) expression in the other sex. Fitness in both sexes follows a sigmoid function of expression  
 135 levels:

$$\begin{aligned}
w_m(E) &= (1 - s_m) + s_m \frac{1}{1 + \exp[-\sigma_m(E - C_m)]} \\
w_f(E) &= (1 - s_f) + s_f \frac{1}{1 + \exp[\sigma_f(E - C_f)]}
\end{aligned}
\tag{2}$$

136

137 where  $w_m(E)$  is male fitness and  $w_f(E)$  is female fitness,  $s$  defines the overall strength of selection,  
138  $\sigma$  determines the steepness of the sigmoid function and  $C$  determines the position of the threshold—  
139 where the contribution of expression to fitness is half its maximum. We can then define

$$c = C_f - C_m \tag{3}$$

140

141 as the curvature of the landscape, so that if  $C_f > C_m$  the average effect of an allele with intermediate  
142 expression  $E = 0.5$  will be beneficial compared to alleles with high ( $E = 1$ ) or low ( $E = 0$ ) expres-  
143 sion. We note that under positive curvature, the fitness landscape displays beneficial dominance  
144 reversal (see [41] for review of dominance reversals), such that heterozygotes with intermediate  
145 expression levels have a net selective advantage relative to homozygotes with either high or low  
146 expression. By contrast, while under negative curvature the fitness landscape displays deleterious  
147 dominance reversal owing to intermediate expression being deleterious on average compared to high  
148 or low expression.

## 149 Results

### 150 A regulatory binding site under SA selection

151 Gene expression is controlled, to a large extent, by transcription regulation, where transcription  
152 factors (TFs) bind to characteristic sequences of DNA (binding sites) upstream of a transcription  
153 start site. TFs up- or down-regulate gene expression, for example by aiding or hindering the  
154 acquisition of RNA polymerase at the transcription start site. The biophysical properties of TF  
155 binding are well understood [30, 32, 33, 34, 35, 36]. Thus, Eq. 1 above describes the expression

156 level,  $E$ , of a gene as a function of: i) the number of nucleotides  $n$  in its TF binding site, ii)  
157 the number of nucleotides  $k$  within the binding site that match the maximum binding affinity  
158 “consensus sequence” for the binding site, and iii) the number of TF proteins  $P$  available to bind  
159 the binding site (Fig. 1). A gene whose expression is under SA selection experiences conflicting  
160 sex-specific pressures on its regulation. Here, we focus on the straightforward case of a somatic gene  
161 whose expression is selected to increase in males and decrease in females (the sign associated with  
162 the selection pressures operating on each sex is arbitrary and identical results would be obtained for  
163 the opposite case). We begin by focusing on a single binding site that up-regulates the expression  
164 of its target, meaning that high affinity binding sites are favored in males and low affinity sites are  
165 favoured in females. Eq. 1 thus provides us with the basis for an empirically grounded genotype-  
166 phenotype map for this system, since it relates the nucleotide sequence at the binding site to the  
167 expression level of the gene under SA selection. We assume that the level of gene expression  $E$   
168 relates to fitness by a sigmoidal function (see Methods, Eq. 2) which increases from  $1 - s_m$  (when  
169  $E = 0$ ) to 1 (when  $E = 1$ , where  $E$  is scaled such that  $E = 1$  represents that maximum expression  
170 level) in males and decreases from 1 (when  $E = 0$ ) to  $1 - s_f$  (when  $E = 1$ ) in females.

171 The relative steepness of male and female fitness functions has important consequences for the  
172 evolutionary dynamics of SA binding site variants. In particular, we must distinguish SA fitness  
173 landscapes with *positive* and *negative* curvature, where curvature is determined by average fitness  
174 at intermediate expression levels (see Methods). Curvature is said to be positive when the average  
175 fitness across males and females of intermediate expression alleles ( $E = 1/2$ ) is greater than the  
176 average fitness of maximum or minimum expression alleles ( $E = 1$  or  $E = 0$ ) and to be negative  
177 when the converse is true (Fig. 1).

178 To begin, we use individual-based simulations (see SI) to determine the equilibrium expression  
179 polymorphism at binding sites in SA fitness landscapes with both positive and negative curvature.  
180 We explore polymorphism as a function of population size  $N$  and binding site length  $n$  (Fig. 2).  
181 Because expression is non-linear in the number of correctly matched nucleotides at a binding site  
182 (Fig. 1 – left), we quantify polymorphism at the expression level rather than at the genetic level.  
183 Specifically, we calculate the absolute difference in expression between the two alleles carried by an  
184 individual, averaged across all individuals (see SI). This measure of “expression polymorphism”,  $p$ ,  
185 is maximized ( $p = 1$ ) when one allele of maximum expression and one allele of minimum expression



186 segregate at equal frequencies in the population, resulting in a maximum frequency of heterozygotes  
187 (0.5) all of which carry two alleles with maximally different expression. Simulating a wide range of  
188 binding site lengths  $1 \leq n \leq 100$  (Fig. 2 – left), we find that landscapes with negative curvature  
189 (where intermediate expression is deleterious on average compared to high or low expression) always  
190 lead to the evolution of high levels of expression polymorphism. Conversely, high levels of expression  
191 polymorphism never evolve in landscapes with positive curvature (where intermediate expression  
192 is on average fitter compared to high or low expression), with the notable exception of the limiting  
193 2-allele case ( $n = 1$ ). This result is particularly notable since fitness landscapes with positive  
194 curvature tend to generate pairs of alleles that display dominance reversal, which has been found  
195 previously to promote maintenance of SA polymorphism [24]. What our results show is that, in  
196 the fitness landscapes associated with regulatory evolution, the same circumstances that lead to  
197 dominance reversal also lead to a minimization of sexually antagonistic fitness variation via fixation  
198 of binding site alleles with intermediate strength. These results hold over a wide range of population  
199 sizes  $10^2 \leq N \leq 10^4$  (Fig. 2 – right).

200 Figure 3 illustrates the intuitive explanation for the effect of fitness landscape curvature, in  
201 terms of the selection gradient experienced by mutations that increase or decrease binding affinity  
202 in a typical binding site of 10 nucleotides. When curvature is negative, polymorphism is favored  
203 between pairs of alleles with intermediate binding strength, *and* the polymorphisms are subject  
204 to divergent selection gradients, with weaker sites favored to get weaker and stronger sites to  
205 get stronger. This results in disruptive selection which generally leads to polymorphism. When  
206 curvature is positive, polymorphism can still sometimes be favored at intermediate expression levels,  
207 but there is no disruptive selection and alleles of intermediate binding strength are maintained. This  
208 is because sexual antagonism can be reduced to the mutual advantage of both sexes by fixing an  
209 allele of intermediate expression that maximises average fitness across males and females. In the  
210 2-allele case landscape curvature does not result in these contrasting dynamics. This is because  
211 when  $n=1$  binding is a binary function of whether or not the binding site matches the consensus  
212 sequence, meaning intermediate binding is not possible. Thus, in this case—even with positive  
213 curvature—polymorphism is maintained.

## 214 Polymorphic displacement in a regulatory cascade

215 We have focused so far on a single binding site at a single target gene. However, most genes are  
216 regulated by multiple binding sites and most regulators are themselves subject to regulation, as  
217 part of a wider regulatory network [42, 43]. This is particularly true for genes involved in sex  
218 determination and sexual differentiation for example, which are frequently arranged in regulatory  
219 cascades [44]. In relation to SA selection, this regulatory connectivity creates the potential for  
220 polymorphism to arise at multiple points in a regulatory cascade, even if only a single downstream  
221 gene is subject to direct SA selection for expression.

222 In order to investigate the invasion and maintenance of SA polymorphism across regulatory  
223 cascades, we once again assume a gene whose expression is under SA selection such that high  
224 expression is favored in males and low expression in females. However, we now assume that this  
225 gene (gene 1) is at the bottom of a three-gene regulatory cascade (Fig. 4c, right), where its expression  
226 is up-regulated by a second (gene 2) which in turn is up-regulated by a third (gene 3). The third  
227 gene further has a binding site that up-regulates its own expression in response to some constant  
228 input signal (see SI).

229 Under a fitness landscape with negative curvature, SA selection on the expression of gene 1  
230 could potentially lead to polymorphism at any of the three binding sites in the cascade. However,  
231 determining precisely where polymorphism will arise is not straightforward, since there is a great  
232 deal of epistasis between mutations at different positions in the cascade, meaning that both the  
233 ordering of mutations as well as their average fitness effects in males and females becomes important  
234 to subsequent evolutionary dynamics [45]. We therefore used simulations to explore the evolutionary  
235 dynamics of all three binding sites (Fig. 4a), starting with a three-gene cascade in which all binding  
236 sites have high affinity ( $k = n$ ). We observe that a high degree of expression polymorphism initially  
237 arises at gene 1, only to subsequently shift towards genes 2 and 3 that sit higher up the cascade.

238 To understand these dynamics, it is first necessary to evaluate why expression polymorphism  
239 should initially arise at the gene directly under SA selection for expression (gene 1). Indeed,  
240 we observe that expression polymorphism almost always initially arises at gene 1 ( $> 90\%$  of cases,  
241 Fig. 4b), and that there is an approximately exponential decline in the frequency of initial expression  
242 polymorphism as we move up the cascade to genes 2 and 3. This pattern can be explained by the

243 buffering properties of regulatory cascades, where changes upstream of a focal gene may only result  
244 in minimal downstream consequences (as long as binding is strong and proteins are reasonably  
245 abundant). Here, this means that mutations to the binding sites of genes 2 and 3 initially generate  
246 little variation in expression of the gene directly under SA selection (gene 1). Accordingly, the  
247 selection gradients operating on these upstream binding sites are comparatively weak and mutant  
248 alleles are unlikely to invade and fix. By contrast, the effects of mutations directly in the binding  
249 site of gene 1 are not buffered by the regulatory cascade, resulting in much larger phenotypic  
250 changes. This means that the strength of selection on the binding site at gene 1 is strong, making  
251 it relatively easier for initial polymorphism to arise here (see SI).

252 Regulatory buffering can not only explain the initial emergence of regulatory polymorphism at  
253 gene 1, it is also central to its subsequent displacement. Specifically, displacement is driven by  
254 advantageous effects of buffering on fitness in heterozygotes. If gene 1 is polymorphic for highly  
255 divergent binding site alleles, such that homozygotes have either expression  $E \approx 1$  or  $E \approx 0$ ,  
256 heterozygotes will have average expression  $E \approx 0.5$  of gene 1. In a fitness landscape with negative  
257 curvature,  $E = 0.5$  yields the lowest possible fitness and the fitness of heterozygotes is maximally  
258 depressed. The emergence of an equivalent polymorphism further upstream in the cascade (gene  
259 2 or gene 3) is then selectively favoured, because it results in heterozygotes expressing at levels  
260  $E > 0.5$  or  $E < 0.5$  (while homozygote expression remains unchanged at  $E \approx 1$  or  $E \approx 0$ ) and  
261 alleviates the fitness costs. Thus, the higher overall fitness associated with expression polymorphism  
262 at upstream genes will precipitate the upwards displacement of polymorphism, away from gene 1.

263 Finally, we find that over long timescales expression polymorphism is most likely to ultimately  
264 reside at the very top of the regulatory cascade (gene 3). This pattern is initially surprising  
265 because there is no mean fitness advantage for expression polymorphism at gene 3 relative to gene  
266 2 (Fig. S4). However, we do observe that the sex-specific fitness of males and females is more similar  
267 when expression polymorphism resides at gene 3 than at gene 2 (Figs. S5 & S6). This suggests that  
268 when there is expression polymorphism at gene 2 there is still disruptive selection that can favour  
269 the invasion of SA alleles further up in the regulatory cascade. Once expression polymorphism is  
270 at gene 3 in the cascade there is greater scope to “fine-tune” the expression level of gene 1 via the  
271 intermediary gene 2, resulting in more balanced male and female fitness, and less opportunity for  
272 disruptive selection.

273 A typical example of polymorphic displacement is shown in Figure 4c. Here, polymorphism  
274 arises quickly at gene 1 before being displaced to gene 3, which remains polymorphic over many  
275 generations. As Figures 4a and 4c both illustrate, displacement takes place over long evolutionary  
276 timescales, with binding sites experiencing around  $10^5$  mutations before any displacement occurs.  
277 We are thus describing a slow and ongoing reorganization of regulatory cascades in response to SA  
278 selection. We note that this phenomenon is expected to be a general feature of landscapes with  
279 negative curvature (see SI).

## 280 Discussion

281 The regulation of gene expression is not only a prime mechanism by which sex-specific adaptation  
282 can be achieved, but also an inevitable target for SA selection. By integrating the population  
283 genetics of SA variants with a biophysical model of transcription factor binding, our study has  
284 generated a number of new predictions for the dynamics of regulatory evolution under SA selection.

285 First, we show that for binding sites of realistic length, SA polymorphisms will only be main-  
286 tained when intermediate expression levels are, on average, deleterious compared to high or low  
287 expression levels. In this scenario of negative curvature, the fitness landscape generates disruptive  
288 selection at intermediate binding that will favor segregating binding site variants of ever more ex-  
289 treme affinities. In contrast, a fitness landscape with positive curvature will favour a monomorphic,  
290 intermediate strength binding site, precluding the maintenance of polymorphism. The requirement  
291 of negative curvature for SA polymorphism only vanishes for the extreme (and unrealistic) case of  
292 binding site length  $n = 1$ , the situation captured by standard 2-allele models of sexual antagonism.  
293 At this limit, mutational effects on TF binding are so coarse that alleles with intermediate expres-  
294 sion cannot arise, and SA polymorphism is predicted even with positive curvature. It is important  
295 to note that our definition of expression polymorphism  $p$  (see SI) measures the variation in termi-  
296 nal gene expression resulting from genetic variation at each locus. This is a highly conservative  
297 measure, which can only reach values  $p \sim 1$  if there is *both* a high level of heterozygosity *and* the  
298 different allelic variants have very different effects on gene expression.

299 Our prediction that fitness landscapes with negative curvature promote SA binding site varia-  
300 tion is in contrast with work focused on 2-allele systems [23, 46, 47], which find that the “positive

301 curvature” scenario and dominance reversal [24] promotes polymorphism. In two allele models,  
302 polymorphism is promoted by effective heterosis, where the fitness of heterozygotes exceeds that  
303 of both homozygotes when measured across sexes [23] and heterozygotes are favoured by selec-  
304 tion. In the system we study, by contrast, polymorphism is the result of disruptive selection on  
305 binding, where intermediate binding strengths are highly deleterious to both sexes (i.e., deleterious  
306 dominance reversal occurs) and heterozygotes are disfavoured by selection. This fundamental dif-  
307 ference makes it difficult to directly compare between the two types of model in how restrictive or  
308 permissive their conditions for polymorphism are.

309 Beyond characterising the conditions under which SA expression variation can occur, our model  
310 allows us to gain insight into the distribution of SA polymorphism across regulatory cascades. Thus,  
311 we predict that allelic variation will be subject to displacement along the regulatory hierarchy.  
312 While polymorphisms are most likely to arise at the target of selection, they can subsequently  
313 move to other genes higher up the regulatory cascade. The ultimate location of polymorphism is  
314 expected to be that which offers the greatest average fitness to heterozygotes while minimising the  
315 opportunity for disruptive selection (see SI). In the type of cascade modeled here, this corresponds  
316 to the gene at the top of the regulatory chain, where buffering of regulatory effects in heterozygotes  
317 results in expression other than  $E = 0.5$  at the target gene and an associated benefit compared  
318 to heterozygotes with strong and weak binding alleles at the target gene. However, it must be  
319 noted that this three-gene cascade is a “minimal complexity” case, and that in reality regulatory  
320 networks involve many more regulators interacting in many more ways. We emphasize the simple  
321 case in order to make it clear that the phenomenon of displaced polymorphism arises even here,  
322 suggesting that in a real network the location of polymorphism arising due to sexual antagonism  
323 will be hard to predict.

324 It is also important to note that the model we present here, as with many other models of sexual  
325 antagonism, focuses on the initial invasion and maintenance of SA alleles. It is widely assumed that  
326 over long timescales, sexual antagonism may be resolved by mechanisms that maintain the benefit  
327 to one sex while removing the cost to the other [48]—ultimately allowing for the restoration of  
328 the optimal phenotype in all individuals. Accordingly, we can only expect to observe polymorphic  
329 displacement in real populations if the timescales over which resolution evolves are more substantial  
330 than those required for displacement to occur. It is currently difficult to say whether that would

331 be expected to be the case, as we still lack empirical data describing the timescales over which  
332 these mechanisms may evolve (although new studies are starting to suggest that the timescales  
333 can indeed be substantial [49]). Moreover, it is evident from our simulations that the timing of  
334 displacement is highly variable. It is therefore reasonable to suppose that whether resolution or  
335 displacement occur first will vary on a case-by-case basis.

336 We predict that SA polymorphism at the top of a cascade will be most beneficial. However,  
337 it is worth noting that this expectation rests on a number of assumptions that do not always  
338 hold in real systems. Our simulations show that the displacement of polymorphism is a highly  
339 stochastic process. Even when assuming strong selection, the fitness differentials that drive upward  
340 displacement rapidly decline along the cascade. Thus, while displacing polymorphism away from  
341 the target gene generates significant gains, the location of polymorphisms in the higher echelons of  
342 the cascade that we observe in our simulations is largely stochastic and dictated by where suitable  
343 mutations first arise. It is likely that this tendency will be exacerbated in real regulatory systems,  
344 where regulatory mutations may have significant pleiotropic effects. As a consequence, it will be  
345 difficult to make precise predictions about the location of polymorphism, other than that it tends  
346 to be above the downstream target gene.

347 A significant factor that will impact displacement is the structure of a regulatory network. Our  
348 simple linear cascade assumes a single target gene under SA selection, yet real-life regulatory net-  
349 works may feature multiple target genes. In cases where all of these target genes are aligned in  
350 terms of the direction of SA selection, such a modular organization may favor and precipitate up-  
351 ward displacement of regulatory polymorphism. This is because, in this case, modularity amplifies  
352 the selective benefits of upstream regulatory variants whose effects propagate across all downstream  
353 target genes. In contrast, co-regulated target genes may be under different types of selection, for ex-  
354 ample, some targets may be under SA selection with others under directional/stabilising selection.  
355 Alternatively, multiple targets may be under SA selection, but in opposing directions. In these  
356 cases, altered regulation of upstream TFs may generate deleterious pleiotropic effects and prevent  
357 polymorphism from being displaced. We may then either see the persistence of SA polymorphism  
358 at individual target genes or larger-scale rewiring of gene regulatory interactions to create modules  
359 of genes under similar selection (see e.g. [50]).

360 The location of SA polymorphism within regulatory networks has consequences for our un-

361 derstanding of how sexual antagonism may be eventually resolved—and hence how sex-specific  
362 development is regulated. The evolution of sex-specific regulation in SA genes is a prime poten-  
363 tial mechanism to achieve resolution, certainly in the case that we consider here, where adaptive  
364 conflict between the sexes occurs over expression levels (rather than coding sequence) of a gene.  
365 As previously discussed, we only expect to observe polymorphic displacement if the timescale for  
366 displacement is shorter than that of resolution. In those cases where polymorphic displacement  
367 precedes resolution, we would expect a corresponding shift in the level at which eventual resolu-  
368 tion may occur. Thus, we would also expect sex-specific regulation to evolve at higher levels of  
369 the regulatory hierarchy than would necessarily occur if resolution was faster than polymorphic  
370 displacement. Reflecting the arguments on modularity above, this should particularly be the case  
371 where genes under SA selection are organised into co-regulated modules. Not only should up-  
372 wards displacement of polymorphism be more strongly selected in these cases, but also its eventual  
373 resolution.

374 Our work has shown that SA selection acting on gene expression can give rise to counter-intuitive  
375 evolutionary dynamics across regulatory networks. These are driven by the conflicting impacts of  
376 the inherent robustness of networks, whereby changes to the expression of an upstream regulator are  
377 frequently compensated for by others downstream. Such buffering tends to prevent the emergence of  
378 initial polymorphism at upstream genes, but once such polymorphism exists at downstream targets,  
379 favors its upward displacement. Over time, we would therefore expect both SA polymorphism and  
380 the sex-specific regulation that may arise to resolve it to reside in the upper reaches of regulatory  
381 networks. Testing these predictions directly is difficult, as current data on SA loci and sex-specific  
382 resolution are relatively sparse. Interestingly, however, parallels exist between sex-specific selection  
383 pressures and directional selection in fluctuating environments [51]. It is therefore plausible that  
384 evolutionary dynamics analogous to those described here occur in networks governing the response  
385 to alternating environmental conditions, allowing the use of microbial evolution for experimental  
386 tests of our theory.

## References

- [1] Rice, W. R., 1984 Sex chromosomes and the evolution of sexual dimorphism. *Evolution* **38**, 735–742. (doi:10.2307/2408385).
- [2] Bonduriansky, R. & Chenoweth, S., 2009 Intralocus sexual conflict. *Trends in ecology and evolution* **24**, 280–288.
- [3] Cox, R. M. & Calsbeek, R., 2009 Sexually antagonistic selection, sexual dimorphism, and the resolution of intralocus sexual conflict. *American Naturalist* **173**, 176–187. (doi:10.1086/595841).
- [4] Pennell, T. M. & Morrow, E. H., 2013 Two sexes, one genome: The evolutionary dynamics of intralocus sexual conflict. *Ecology and Evolution* **3**, 1819–1834. (doi:10.1002/ece3.540).
- [5] Mokkonen, M., Kokko, H., Koskela, E., Lehtonen, J., Mappes, T., Martiskainen, H. & Mills, S. C., 2011 Negative Frequency-Dependent Selection of Sexually Antagonistic Alleles in *Myodes glareolus*. *Science* **334**, 972–974. (doi:10.1126/science.1208708).
- [6] Tarka, M., Åkesson, M., Hasselquist, D., Hansson, B., Akesson, M., Hasselquist, D. & Hansson, B., 2014 Intralocus Sexual Conflict over Wing Length in a Wild Migratory Bird. *American Naturalist* **183**, 62–73. (doi:10.1086/674072).
- [7] Svensson, E. I., McAdam, A. G. & Sinervo, B., 2009 Intralocus sexual conflict over immune defense, gender load, and sex-specific signaling in a natural lizard population. *Evolution* **63**, 3124–3135. (doi:10.1111/j.1558-5646.2009.00782.x).
- [8] Rice, W. R., 1992 Sexually antagonistic genes: experimental evidence. *Science* **256**, 1436–1439. ISSN 0036-8075. (doi:10.1126/science.1604317).
- [9] Berger, D., Berg, E. C., Widegren, W., Arnqvist, G. & Maklakov, A. A., 2014 Multivariate intralocus sexual conflict in seed beetles. *Evolution* **68**, 3457–3469.
- [10] Barson, N. J., Aykanat, T., Hindar, K., Baranski, M., Bolstad, G. H., Fiske, P., Jacq, C., Jensen, A. J., Johnston, S. E., Karlsson, S. *et al.*, 2015 Sex-dependent dominance at a single locus maintains variation in age at maturity in salmon. *Nature* **000**, 1–4.



- 413 [11] Delph, L. F., Andicoechea, J., Steven, J. C., Herlihy, C. R., Scarpino, S. V. & Bell, D. L., 2011  
414 Environment-dependent intralocus sexual conflict in a dioecious plant. *New Phytologist* **192**,  
415 542–552.
- 416 [12] Rice, W. R., 1987 The Accumulation of Sexually Antagonistic Genes as a Selective Agent  
417 Promoting the Evolution of Reduced Recombination between Primitive Sex Chromosomes.  
418 *Evolution* **41**, 9–11.
- 419 [13] Charlesworth, D. & Charlesworth, B., 2005 Sex Chromosomes: Evolution of the Weird and  
420 Wonderful. *Current Biology* **15**, R129–R131.
- 421 [14] Haag, E. S. & Doty, A. V., 2005 Sex determination across evolution: Connecting the dots.  
422 *PLoS Biology* **3**, e21. ISSN 15449173. (doi:10.1371/journal.pbio.0030021).
- 423 [15] Van Doorn, G. S., 2009 Intralocus sexual conflict. *Annals of the New York Academy of Sciences*  
424 **1168**, 52–71. ISSN 00778923. (doi:10.1111/j.1749-6632.2009.04573.x).
- 425 [16] Muralidhar, P. & Veller, C., 2018 Sexual antagonism and the instability of environmental sex  
426 determination. *Nature Ecology & Evolution* **2**, 343–351. ISSN 2397-334X. (doi:10.1038/s41559-  
427 017-0427-9).
- 428 [17] Pischedda, A., Chippindale, A. K., Bangham, J., Rowe, L. & Gocayne, J., 2006 Intralocus  
429 Sexual Conflict Diminishes the Benefits of Sexual Selection. *PLoS Biology* **4**, e356.
- 430 [18] Pennell, T. M., de Haas, F. J. H., Morrow, E. H. & van Doorn, G. S., 2016 Contrasting effects  
431 of intralocus sexual conflict on sexually antagonistic coevolution. *Proc Natl Acad Sci U S A*  
432 **113**, E978–86. (doi:10.1073/pnas.1514328113).
- 433 [19] Patten, M. M., Haig, D. & Úbeda, F., 2010 Fitness variation due to sexual antagonism and  
434 linkage disequilibrium. *Evolution* **64**, 3638–3642. (doi:10.1111/j.1558-5646.2010.01100.x).
- 435 [20] Foerster, K., Coulson, T., Sheldon, B. C., Pemberton, J. M., Clutton-Brock, T. H. & Kruuk,  
436 L. E. B., 2007 Sexually antagonistic genetic variation for fitness in red deer. *Nature* **447**,  
437 1107–1110. (doi:10.1038/nature05912).

- 438 [21] Dutoit, L., Mugal, C. F., Bolívar, P., Wang, M., Nadachowska-Brzyska, K., Smeds, L., Yazdi,  
439 H. P., Gustafsson, L. & Ellegren, H., 2018 Sex-biased gene expression, sexual antagonism and  
440 levels of genetic diversity in the collared flycatcher ( *Ficedula albicollis* ) genome. *Molecular*  
441 *Ecology* **27**, 3572–3581. ISSN 09621083. (doi:10.1111/mec.14789).
- 442 [22] Kirkpatrick, M., 2009 Patterns of quantitative genetic variation in multiple dimensions. *Ge-*  
443 *netica* **136**, 271–284. ISSN 00166707. (doi:10.1007/s10709-008-9302-6).
- 444 [23] Kidwell, J. F., Clegg, M. T., Stewart, F. M. & Prout, T., 1977 Regions of stable equilibria for  
445 models of differential selection in the two sexes under random mating. *Genetics* **85**, 171–183.  
446 ISSN 00166731.
- 447 [24] Fry, J. D., 2010 The genomic location of sexually antagonistic variation: Some cautionary  
448 comments. *Evolution* **64**, 1510–1516. ISSN 00143820.
- 449 [25] Mullan, C., Pomiankowski, A. & Reuter, M., 2012 The effects of selection and genetic drift  
450 on the genomic distribution of sexually antagonistic alleles. *Evolution* **66**, 3743–3753. ISSN  
451 00143820. (doi:10.1111/j.1558-5646.2012.01728.x).
- 452 [26] Connallon, T. & Clark, A. G., 2012 A general population genetic framework for antagonistic  
453 selection that accounts for demography and recurrent mutation. *Genetics* **190**, 1477–1489.  
454 ISSN 00166731. (doi:10.1534/genetics.111.137117).
- 455 [27] Connallon, T., Sharma, S. & Olito, C., 2018 Evolutionary Consequences of Sex-Specific Selec-  
456 tion in Variable Environments: Four Simple Models Reveal Diverse Evolutionary Outcomes.  
457 *The American Naturalist* **193**, 93–105. ISSN 0003-0147. (doi:10.1086/700720).
- 458 [28] Úbeda, F., Haig, D. & Patten, M. M., 2011 Stable linkage disequilibrium owing to sexual  
459 antagonism. *Proceedings of the Royal Society B: Biological Sciences* **278**, 855–862. ISSN  
460 14712970. (doi:10.1098/rspb.2010.1201).
- 461 [29] Lande, R., 1980 Sexual dimorphism, sexual selection, and adaptation in polygenic characters.  
462 *Evolution* **34**, 292–305. (doi:10.2307/2407393).
- 463 [30] Gerland, U. & Hwa, T., 2002 On the selection and evolution of regulatory DNA motifs. *Journal*  
464 *of Molecular Evolution* **55**, 386–400. ISSN 00222844. (doi:10.1007/s00239-002-2335-z).

- 465 [31] Lässig, M., 2007 From biophysics to evolutionary genetics: statistical aspects of gene regula-  
466 tion. *BMC Bioinformatics* **8**, S7. ISSN 14712105. (doi:10.1186/1471-2105-8-S6-S7).
- 467 [32] Buchler, N. E., Gerland, U. & Hwa, T., 2003 On schemes of combinatorial transcription logic.  
468 *Proceedings of the National Academy of Sciences of the United States of America* **100**, 5136–41.  
469 ISSN 0027-8424. (doi:10.1073/pnas.0930314100).
- 470 [33] Bintu, L., Buchler, N. E., Garcia, H. G., Gerland, U., Hwa, T., Kondev, J. & Phillips, R.,  
471 2005 Transcriptional regulation by the numbers: Models. *Current Opinion in Genetics and*  
472 *Development* **15**, 116–124. ISSN 0959437X. (doi:10.1016/j.gde.2005.02.007).
- 473 [34] Mustonen, V., Kinney, J., Callan, C. G. & Lässig, M., 2008 Energy-dependent fitness: a  
474 quantitative model for the evolution of yeast transcription factor binding sites. *Proceedings of*  
475 *the National Academy of Sciences of the United States of America* **105**, 12376–12381. ISSN  
476 1091-6490. (doi:10.1073/pnas.0805909105).
- 477 [35] Stewart, A. J., Hannehalli, S. & Plotkin, J. B., 2012 Why transcription factor binding sites  
478 are ten nucleotides long. *Genetics* **192**, 973–85. (doi:10.1534/genetics.112.143370).
- 479 [36] Tuğrul, M., Paixão, T., Barton, N. H. & Tkačik, G., 2015 Dynamics of transcription factor  
480 binding site evolution. *PLoS Genet* **11**, e1005639. (doi:10.1371/journal.pgen.1005639).
- 481 [37] Lynch, M. & Conery, J., 2003 The origins of genome complexity. *Science* **302**, 1401.
- 482 [38] Sella, G. & Hirsh, A. E., 2005 The application of statistical physics to evolutionary biology.  
483 *Proceedings of the National Academy of Sciences of the United States of America* **102**, 9541–6.  
484 ISSN 0027-8424. (doi:10.1073/pnas.0501865102).
- 485 [39] Lemos, B., Araripe, L. O., Fontanillas, P. & Hartl, D. L., 2008 Dominance and the evolutionary  
486 accumulation of cis- and trans-effects on gene expression. *Proceedings of the National Academy*  
487 *of Sciences* **105**, 14471–14476. ISSN 0027-8424. (doi:10.1073/pnas.0805160105).
- 488 [40] McManus, C. J., Coolon, J. D., Duff, M. O., Eipper-Mains, J., Graveley, B. R. & Wittkopp,  
489 P. J., 2010 Regulatory divergence in *Drosophila* revealed by mRNA-seq. *Genome Research*  
490 **20**, 816–825. ISSN 10889051. (doi:10.1101/gr.102491.109).

- 491 [41] Connallon, T. & Chenoweth, S. F., 2019 Dominance reversals and the maintenance of  
492 genetic variation for fitness. *PLOS Biology* **17**, e3000118. ISSN 1545-7885. (doi:  
493 10.1371/journal.pbio.3000118).
- 494 [42] Stewart, A. J., Seymour, R. M. & Pomiankowski, A., 2009 Degree dependence in rates of tran-  
495 scription factor evolution explains the unusual structure of transcription networks. *Proceedings*  
496 *of the Royal Society B: Biological Sciences* **276**, 2493–501. (doi:10.1098/rspb.2009.0210).
- 497 [43] Stewart, A. J. & Plotkin, J. B., 2013 The evolution of complex gene regulation by low-specificity  
498 binding sites. *Proceedings of the Royal Society B: Biological Sciences* **280**, 20131313. (doi:  
499 10.1098/rspb.2013.1313).
- 500 [44] Herpin, A. & Scharfl, M., 2015 Plasticity of gene-regulatory networks controlling sex deter-  
501 mination: of masters, slaves, usual suspects, newcomers, and usurpators. *EMBO reports* **16**,  
502 1260–1274. ISSN 1469-221X. (doi:10.15252/embr.201540667).
- 503 [45] Shah, P., McCandlish, D. M. & Plotkin, J. B., 2015 Contingency and entrenchment in pro-  
504 tein evolution under purifying selection. *Proc Natl Acad Sci U S A* **112**, E3226–35. (doi:  
505 10.1073/pnas.1412933112).
- 506 [46] Patten, M. M. & Haig, D., 2009 Maintenance or loss of genetic variation under sexual and  
507 parental antagonism at a sex-linked locus. *Evolution* **63**, 2888–2895.
- 508 [47] Connallon, T. & Clark, G. A., 2011 The resolution of sexual antagonism by gene duplication.  
509 *Genetics* **187**, 919–937.
- 510 [48] Stewart, A. D., Pischedda, A. & Rice, W. R., 2010 Resolving intralocus sexual conflict: Genetic  
511 mechanisms and time frame. *Journal of Heredity* **101**, S94–9. (doi:10.1093/jhered/esq011).
- 512 [49] Ruzicka, F., Hill, M. S., Pennell, T. M., Flis, I., Ingleby, F. C., Mott, R., Fowler, K., Morrow,  
513 E. H. & Reuter, M., 2019 Genome-wide sexually antagonistic variants reveal long-standing  
514 constraints on sexual dimorphism in fruit flies. *PLOS Biology* **17**, e3000244. ISSN 1545-7885.  
515 (doi:10.1371/journal.pbio.3000244).
- 516 [50] Tsong, A. E., Tuch, B. B., Li, H. & Johnson, A. D., 2006 Evolution of alternative transcrip-  
517 tional circuits with identical logic. *Nature* **443**, 415–20. (doi:10.1038/nature05099).

518 [51] Reuter, M., Camus, M. F., Hill, M. S., Ruzicka, F. & Fowler, K., 2017 Evolving plastic re-  
519 sponses to external and genetic environments. *Trends in Genetics* **33**, 169–170. ISSN 13624555.  
520 (doi:10.1016/j.tig.2017.01.004).

521 [52] Kimura, M. & Crow, J., 1964 The number of alleles that can be maintained in a finite popu-  
522 lation. *Genetics* **49**, 725–738.

523 **Acknowledgments**

524 This work was supported by a UCL IMPACT PhD Studentship to M. S. H. and a Royal Society  
525 University Research Fellowship to A. J. S.

526 **Author contributions**

527 M. S. H., M. R., & A. J. S. designed the project, M. S. H. & A. J. S. conducted analyses and  
528 produced figures. All authors interpreted the results and contributed to writing of the manuscript.

529 **Competing interests**

530 The authors declare no competing interests.

## 531 **Figure Legends**

532 **Figure 1: Sexually antagonistic selection on gene expression.** Regulation of gene expression  
533 by TF binding sites is well understood at a mechanistic level, allowing us to construct explicit  
534 genotype-phenotype maps. In the case we consider, expression level  $E$  increases with the number  
535 of nucleotides  $k$  correctly matched to a consensus sequence (left). Binding site length  $n$  is well  
536 known to have important consequences for the dynamics of binding site evolution [36, 35] generally.  
537 However, population genetic models of sexual antagonism typically focus either on a 2-allele system  
538 [23, 1, 24, 25, 26] (corresponding to a binding site of 1nt in length), or in some contexts on the  
539 continuum limit and infinite alleles [52]. Eukaryotic TF binding sites, in contrast, are typically  
540 around 10 nucleotides long [35], and vary from as short as 5nt to  $> 20$ nt in some cases. By varying  
541 the binding site length  $n$  and characterizing a binding site by the number of matched nucleotides  $k$   
542 we can generate a system with as few as 2-alleles (top - left) to an infinite number of alleles in the  
543 continuum limit (bottom - left). A realistic eukaryotic TF binding site length of  $n = 10$ nt results  
544 in 11 alleles at a given locus. We assume that expression is selected to be high in males (blue)  
545 and low in females (red) (right), and we consider fitness landscapes with different “curvatures”  
546 corresponding to different levels of average fitness at intermediate expression levels.

547 **Figure 2: Expression polymorphism at a single binding site.** Results of individual based  
548 simulations showing the amount of polymorphism in gene expression ( $p$  – see SI) as a function of  
549 (left) binding site length  $n$ , where we construct a single binding site with length varying from 1  
550 (below the observed range of real binding site lengths) to 100 nucleotides (well above the observed  
551 range of real binding site lengths) and calculate expression from Eq. 1. and (right) population size  
552  $N$  for landscapes with negative (dark gray) and positive (light gray) curvature. Points show the  
553 ensemble average of  $10^4$  runs at each parameter value. Default population size was fixed at  $N = 10^3$   
554 and default binding site length at  $n = 10$ . Per-binding site mutation rates were set to  $N_e\mu = 0.1$ ,  
555 selection was assumed to be strong ( $s_m = s_f = 0.1$ ). Curvature was set to  $c = \pm 0.2$  and the fitness  
556 landscape had steepness  $h = 10$  (see Methods). Each simulation was run until  $10^6$  mutations per  
557 binding site had occurred.

558 **Figure 3: Pairwise invasion plot for a single binding site.** We calculated the selection

559 gradient (see SI) for a “typical” binding site of 10 nucleotides, assuming weak mutation so that  
560 at most two alleles segregate in a population at a given time, as a function of fitness landscape  
561 curvature  $c$ . We also used a two-allele approximation to determine whether polymorphism was  
562 favored (see SI for details), with the polymorphic region indicated in dark gray. Solid purple  
563 lines indicate stable monomorphic equilibria that arise due to mutation and drift while dashed  
564 lines indicate unstable equilibria. Blue arrows indicate the direction of the selection gradient  
565 on an invading allele that benefits males and red the direction of selection on an invading allele  
566 benefiting females. Black arrows indicate the direction of evolution in a monomorphic population  
567 under antagonistic selection. Note that when curvature is negative (left hand side,  $c < 0$ ) the  
568 evolutionary dynamics lead to convergence on the intermediate, unstable equilibrium. Once this  
569 has been reached, the population experiences disruptive selection, a scenario that results in the  
570 emergence and maintenance of SA polymorphism. When curvature is positive (right hand side  
571  $c > 0$ ) the evolutionary dynamics also converge on the intermediate equilibrium, but since this is  
572 stable, with males and females both experiencing high fitness, polymorphism is limited and sexual  
573 antagonism is minimal.

574 **Figure 4: Displaced polymorphism in a regulatory cascade under a fitness landscape**  
575 **with negative curvature.** a) We observed the average expression polymorphism for each gene  
576 over evolutionary time. The initial phase (inset) sees expression polymorphism arise at gene 1  
577 (yellow) and beginning to pass to gene 2 (red) and gene 3 (blue) higher up the cascade. b) We  
578 determined where in the cascade expression polymorphism of  $p > 0.5$  first arose. In  $> 90\%$  of  
579 simulation runs expression polymorphism initially arises at gene 1, with the frequency declining  
580 approximately exponentially with position in the cascade. c) A sample path for a single simulation  
581 run shows the dynamics of displacement explicitly, with gene 1 quickly acquiring polymorphism  
582 until a displacement event shifts the polymorphism up the chain to gene 3. Shading indicates allele  
583 frequencies within the population. These individual based simulations for a cascade of three genes  
584 were carried out using the same default parameters given in Figure 2.



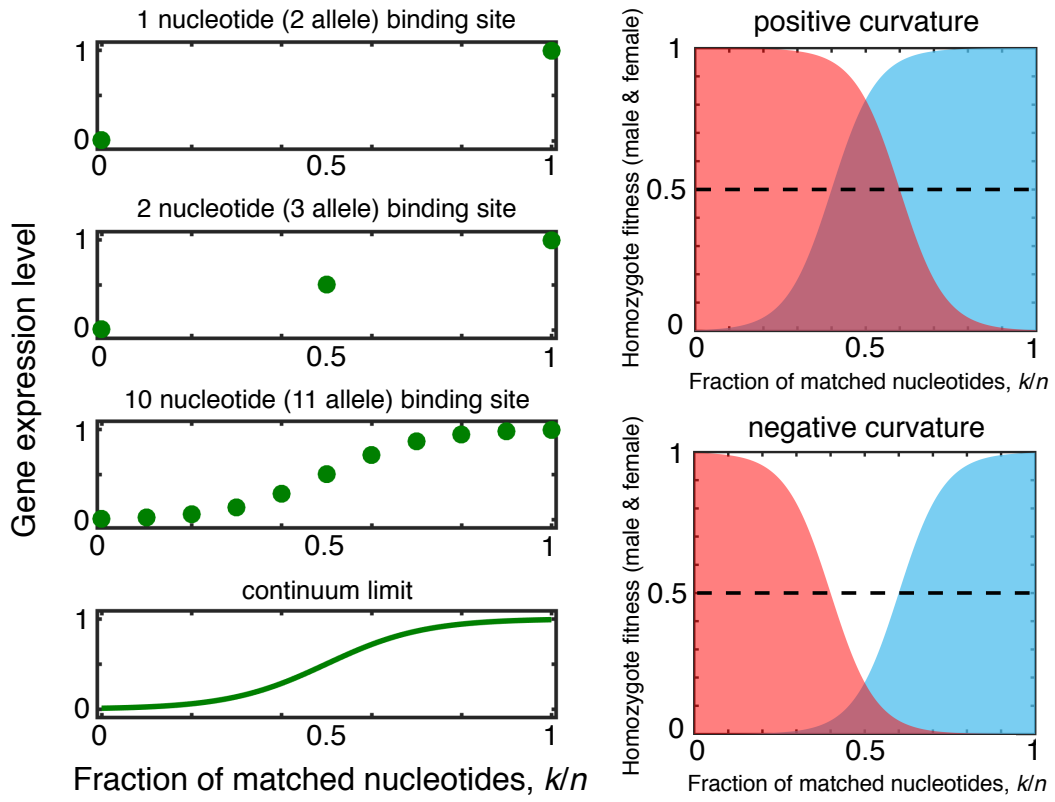


**Figure 1: Sexually antagonistic selection on gene expression.**

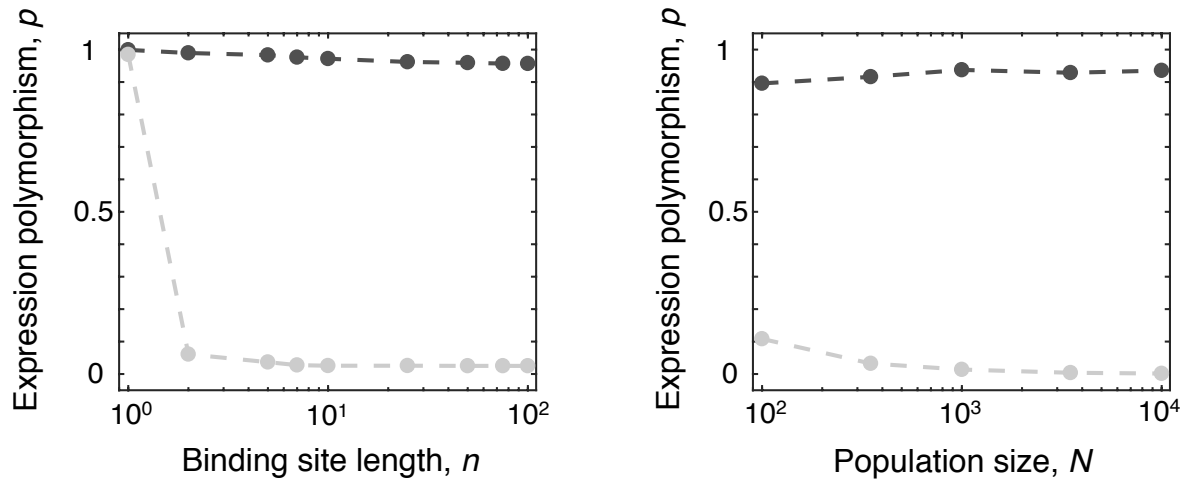


Figure 2: Expression polymorphism at a single binding site.

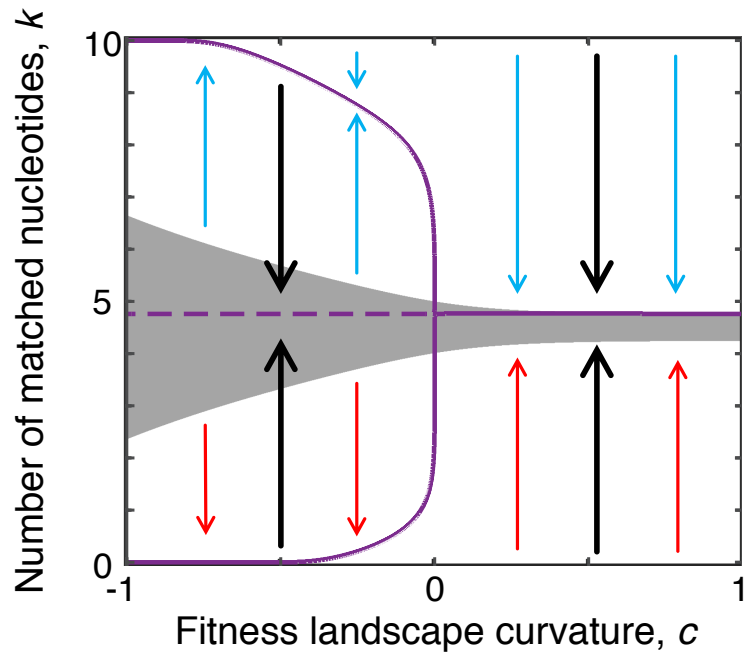


Figure 3: Pairwise invasion plot for a single binding site.

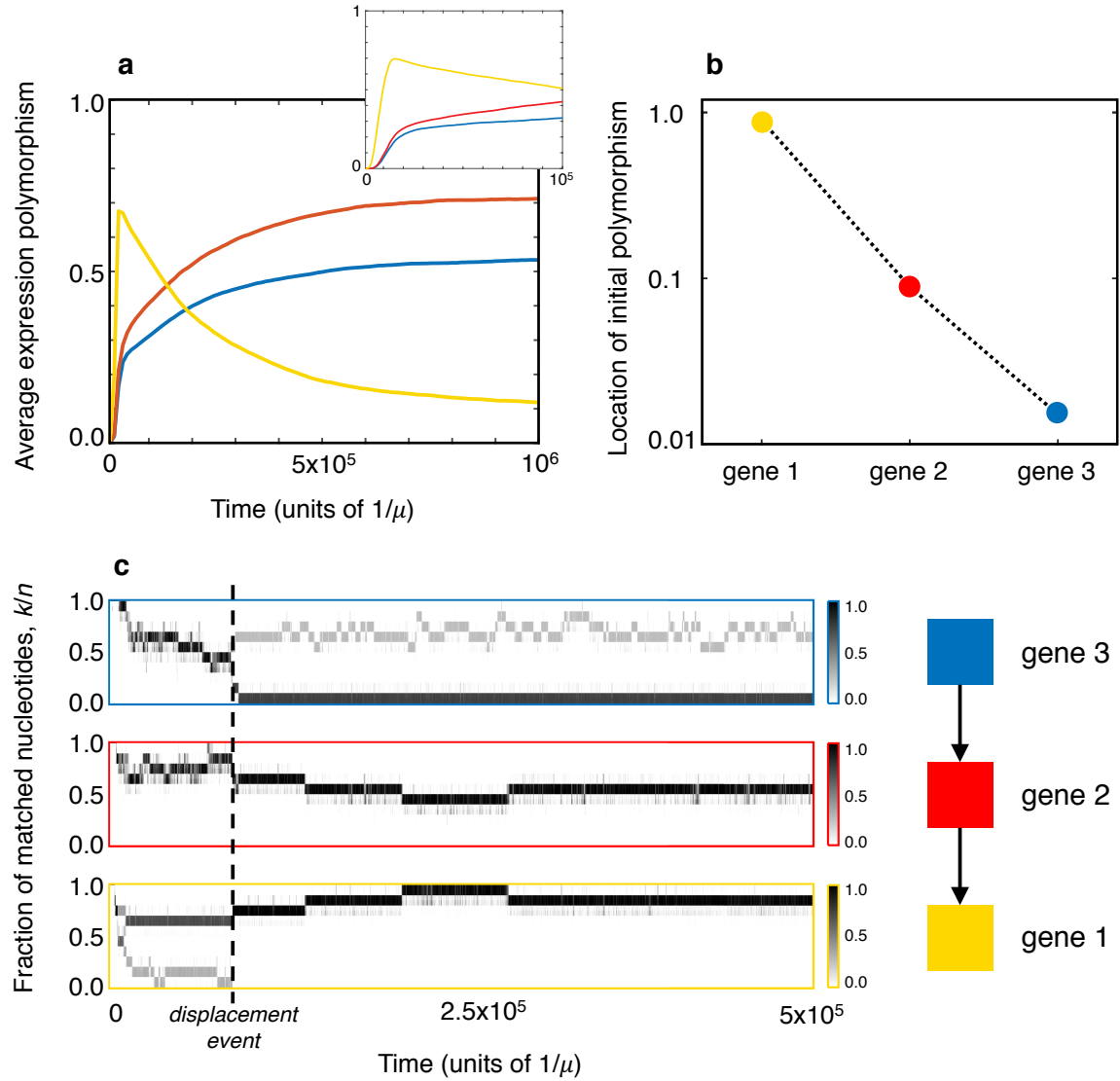


Figure 4: Displaced polymorphism in a regulatory cascade under a fitness landscape with negative curvature.